J Mater Sci: Mater Med (2010) 21:1829–1835
DOI 10.1007/s10856-010-4059-8

A study on mineralization behavior of amino-terminated hyperbranched polybenzimidazole membranes

Xiayun Huang · Hongcui Cao · Zixing Shi · Hongjie Xu · Jianhua Fang · Jie Yin · Qiaoling Pan

Received: 12 July 2009 / Accepted: 15 March 2010 / Published online: 7 April 2010

Abstract Amino-bearing polymers, coated with apatite or similar minerals, have attracted significant attention for their potential in medical applications. In this study, an amino-terminated hyperbranched polybenzimidazole (HBPBI) membrane was used as a substrate for apatite growth. The membrane was soaked in solutions of $CaCl_2$, Na_2HPO_4 and SBF to yield an apatite coating. The structure and morphology of the layers were characterized by FTIR-ATR, XRD and FESEM. The results indicate that the high densities of amino, imide and imidazole groups on the amino-terminated HBPBI membrane provide active sites for the growth of apatite.

1 Introduction

The biological affinity and protein adsorption characteristics of apatite make it a useful mineral in biology and medicine [1]. Apatite deposited onto the surface of organic polymers provides a potential matrix for tissue repair [1–3]. Various polymeric materials have been used as substrates for apatite growth, including natural materials, like silk [4], protein [5–7], and chitosan hydrogel [8]; biodegradable materials, such as poly(ε-caprolactone) (PCL) [9, 10], polylactic-co-glycolic acid (PDLA) scaffold [11, 12], and polyamide (PA) [13, 14]; and non-biodegradable materials, like polyethylene (PE) [15, 16], poly(vinyl alcohol) (PVA) [17], and poly(methylmethacrylate) (PMMA) [18]. Most of these substrates were functionalized with negatively charged groups, such as phosphates ($–PO_4H_2$) [19], sulfonic acids ($–SO_3H$) [13], carboxylic acids (–COOH) [10, 20], and hydroxyl groups (-OH) [17], to facilitate apatite nucleation [21, 22].

It is generally believed that polymers bearing only amino groups are less active for apatite growth than those bearing negatively charged groups. This has been attributed to the protonation of amino groups in acidic $CaCl_2$ solution, which slows the growth of apatite layers. Thus, carboxylic acids are usually incorporated to effectively increase the rate of apatite nucleation.

The current study describes an alternative method of accelerating nucleation on amino-bearing polymers. The hyperbranched structure of an amino-terminated HBPBI membrane provides a high density of nitrogenous functional groups, including primary amine, imide and imidazole groups, to accelerate the rate of apatite nucleation [23]. Additionally, the excellent mechanical properties, thermal stability and chemical resistance [24–26] of the amino-terminated HBPBI membrane make this apatite-coated composite especially useful as a potential scaffold for biomedical applications or as an absorbent for removing volatile organic compounds (VOCs) [27].

The amino-terminated HBPBI [28, 29] membrane was prepared as previously reported. Apatite was grown on the membrane using a two-step soaking procedure. The

X. Huang · Z. Shi (✉) · H. Xu · J. Fang · J. Yin
School of Chemistry and Chemical Engineering, Shanghai Jiao Tong University, 800 Dongchuan Road, Shanghai 200240, People's Republic of China
e-mail: zxshi@sjtu.edu.cn

H. Cao (✉) · Q. Pan
State Key Laboratory for Diagnosis and Treatment of Infectious Diseases, 1st Affiliated Hospital, College of Medicine, Zhejiang University, 79, Qingchun Road, Hangzhou 310003, People's Republic of China
e-mail: caohc70@yahoo.com.cn

J. Yin
State Key Labroatory of Metal Matrix Composites, Shanghai Jiao Tong University, 800 Dongchuan Road, Shanghai 200240, People's Republic of China

membranes were first alternatively soaked in solutions of $CaCl_2$ and Na_2HPO_4 for 15 cycles. Second, the membranes were immersed in SBF solution. The growth of apatite on the amino-terminated HBPBI membranes was characterized by FTIR-ATR, XRD and FESEM. The results indicated that the amino, imide and imidazole groups of the amino-terminated HBPBI membranes provided active sites for apatite nucleation. In the first step of the deposition process, the imidazole groups likely coordinated calcium ions to induce the nucleation. In the second step, amino and imide groups interacted with phosphate ions to facilitate apatite formation.

2 Materials and methods

2.1 Materials

3,3′-Diaminobenzidine (DAB), iso-phthalic acid (*i*PTA) and 1,3,5-benzenetricarboxylic acid (BTA) were purchased from Acros and were used without further purification. Terephthaldehyde (TPA), phosphorous pentoxide (P_2O_5), polyphosphoric acid (PPA), and dimethylsulfoxide (DMSO) were purchased from SCRC. DMSO was distilled under reduced pressure and dried over 4A molecular sieves before use. Disodium hydrogen phosphate (Na_2HPO_4), calcium chloride ($CaCl_2$) and tris (hydroxymethyl) aminomethane (Tris) were also purchased from SCRC.

2.2 Preparation of amino-terminated HBPBI membranes

Amino-terminated HBPBI membranes were prepared as described in References [28] and [29]. This synthesis involved two stages, as shown in Scheme 1. In the first stage, 4 mmol DAB was added to 130 g PPA, containing 85%, P_2O_5 under a nitrogen flow. After the DAB was completely dissolved, 2 mmol *i*PTA was added in three portions. The mixture was mechanically stirred at 150°C for 2 h. The reaction temperature was then raised to 190°C and maintained for 20 h to yield the tetramine monomer. In the second stage, the reaction mixture was allowed to cool to room temperature, and 1 mmol BTA was added in three portions. The mixture was mechanically stirred at 150°C for 2 h after each addition of BTA. The reaction temperature was then raised to 190°C and maintained for 20 h. The reaction mixture was cooled to room temperature, mixed with ice water, neutralized with ammonium hydroxide and filtered. The solid was further extracted with 10% ammonium hydroxide in a Soxhlet apparatus for 24 h, thoroughly washed with deionized water, and dried under reduced pressure at 60°C for 20 h to obtain amino-terminated HBPBI.

Amino-terminated HBPBI membranes were prepared by casting a solution of the above polymer mixed with a crosslinker, terephthaldehyde (TPA), into a thin membrane, as shown in Scheme 1. The thickness of the membranes was around 30 μm. The membranes were cut into 2 cm × 2 cm pieces. Membranes were pretreated by soaking in 1 mol/l hydrochloric acid at 50°C for 10 h, followed by thorough washing with deionized distilled water. The membranes were then soaking in deionized water at 50°C for 48 h prior to apatite deposition.

2.3 Preparation of apatite coating on amino-terminated HBPBI membranes

An apatite coating on the above amino-terminated HBPBI membranes was created as shown in Scheme 2. First, the amino-terminated HBPBI membranes were alternately immersed in solutions of Ca (200 mM $CaCl_2$) and P

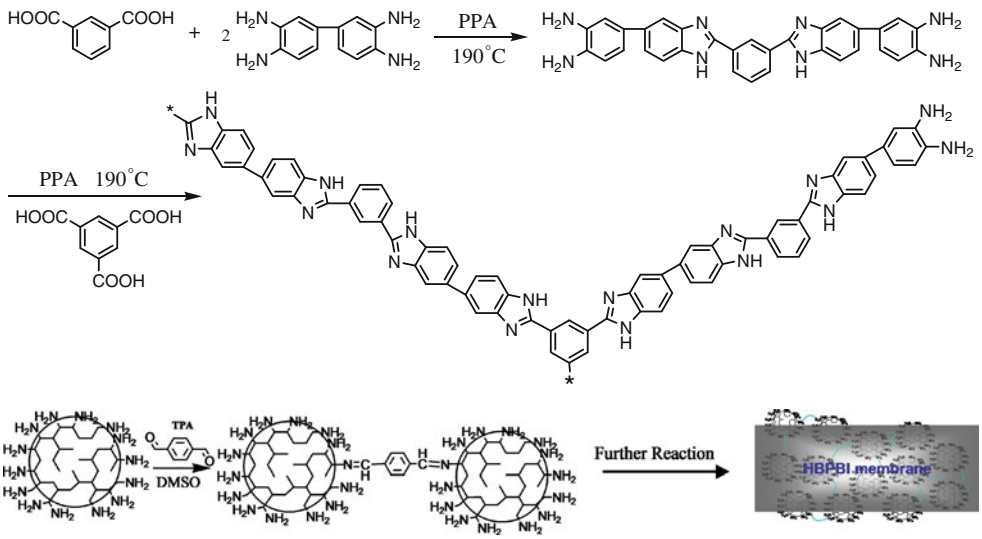

Scheme 1 Synthesis of amino-terminated HBPBI membranes

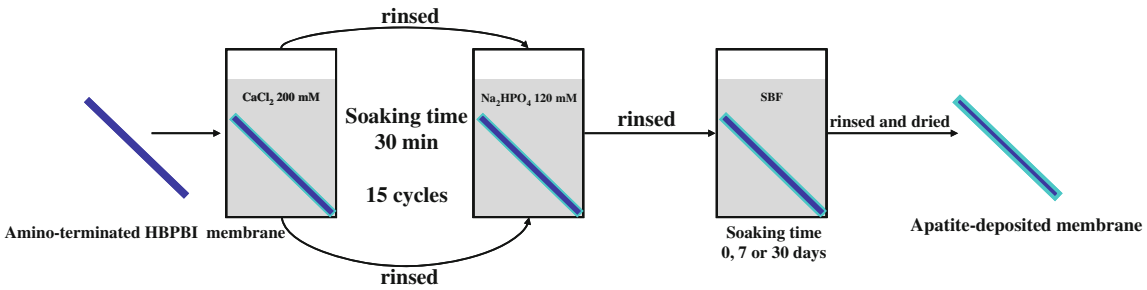

Scheme 2 Preparation of apatite-coated amino-terminated HBPBI membranes

(120 mM Na_2HPO_4) for 15 cycles. A step-wise description of this process follows:

Step 1: HBPBI membranes (2 cm × 2 cm) were soaked in 100 ml of aqueous $CaCl_2$ (200 mM) (Ca solution) at 36.5°C for 30 min.
Step 2: The membranes were removed from the Ca solution, and rinsed copiously with deionized distilled water at 36.5°C for approximately 10 s to remove residual Ca solution from the membrane surface. Excess moisture was removed by blotting with filter paper.
Step 3: The membrane was then soaked in 100 ml of aqueous Na_2HPO_4 (120 mM) (P solution) at 36.5°C for 30 min.
Step 4: The membrane was again rinsed and blotted as described in Step 2.

This process was repeated for 15 times. The membranes were then removed from solution, gently washed with deionized distilled water and air-dried for 24 h. The obtained samples were designated "HBPBI-15".

The HBPBI-15 membranes were immersed individually in 100 ml of SBF solution refreshed every 24 h SBF solution was prepared by dissolving reagent grade NaCl, $NaHCO_3$, KCl, $K_2HPO_4{\cdot}3H_2O$, $MgCl_2{\cdot}6H_2O$, $CaCl_2$, Na_2SO_4 in deionized distilled water to yield the following ion concentrations: Na^+ 142.0, K^+ 5.0, Mg^{2+} 1.5, Ca^{2+} 2.5, Cl^- 103.0, HCO^{3-} 27.0, $HPO_4{}^{2-}$ 1.0, $SO_4{}^{2-}$ 0.5 mM) [30]. The pH of the SBF solution was buffered at 7.40 at 36.5°C by the addition of tris (hydroxymethyl) amino-methane and an appropriate volume of hydrochloric acid. After soaking for 7 or 30 days, membranes were removed from the SBF solution, washed with deionized distilled water, and dried at the room temperature for 24 h. The resulting membranes are referred to as HBPBI-15-7 and HBPBI-15-30, respectively.

2.4 Characterization

The chemical structure of the apatite coating was examined by Fourier-transform infrared attenuated total internal reflection spectroscopy (FTIR-ATR) using the multiple reflection mode on a Nexus 670 instrument (Nicolet Corporation, USA). The experiments were carried out at room temperature in dry air. The apatite phase was evaluated by X-ray powder diffraction (XRD: D/max-2200/PC, Japan Rigaku Corporation) using a Cu K_α source operating at 40 kV and 50 mA. The structure of the apatite was also analyzed with a field emission transmission electron microscope (FETEM: JEOL 2100F, JEOL Ltd., Japan) equipped with an energy dispersive spectroscopy attachment (EDX: Oxford, England) operating at 200 kV. The apatite was scraped from the membrane, dispersed in ethanol, deposited onto carbon-coated copper grids, and dried at room temperature. Surface microstructures of the coated membranes were observed with an optical microscope (POM: Leica DM LP, Leica Microsystems GmbH, Germany) and field emission scanning electron microscope (FESEM; JSM-7401F, JEOL Ltd., Japan).

3 Results

Optical microscopy images were acquired periodically during the soaking process to follow the changes in the surface morphology of the amino-terminated HBPBI membrane. Figure 1b show apatite precursors on the otherwise smooth surface of the amino-terminated HBPBI membranes, after 15 cycles alternate soaking. Figure 1c and d show that further soaking in the SBF solution for 7 or 30 days, respectively, resulted in denser coverage of apatite crystals.

The FESEM images in Fig. 2 show the growth of apatite on the amino-terminated HBPBI membranes as a function of soaking time. After several alternate soaking cycles, the membrane surface was covered with multiple layers of the apatite coating, consisting of complete planar sublayers and partial flower-like top layers. The sublayers were aligned vertically along the *c* axis with plate-shaped apatite crystals assembled in a layer-by-layer manner. The small flower-like top layers were also clustered by the plate-shaped apatite crystals, which may serve as secondary nucleation

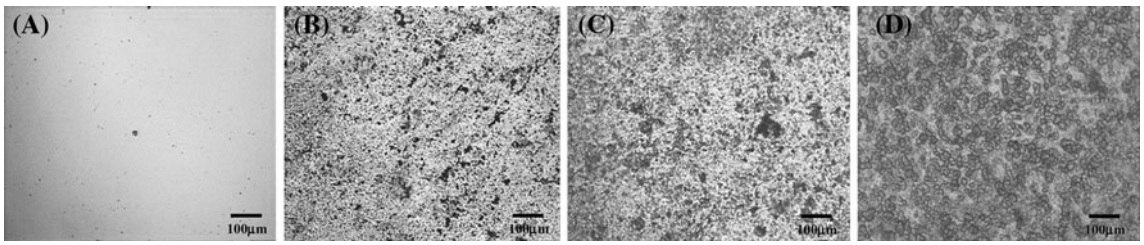

Fig. 1 Optical micrographs showing the surface morphology of **a** pure HBPBI, **b** HBPBI-15, **c** HBPBI-15-7 and **d** HBPBI-15-30 membranes

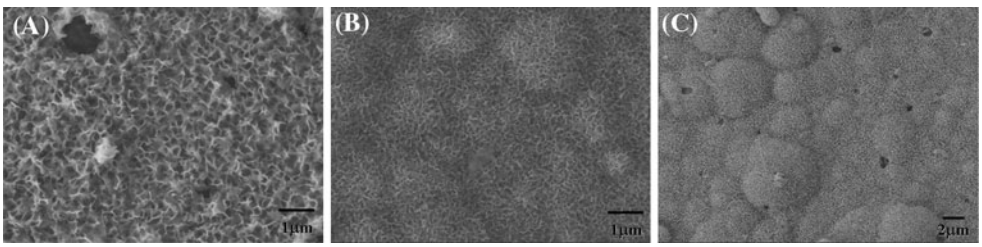

Fig. 2 FESEM images of apatite coatings on **a** HBPBI-15, **b** HBPBI-15-7 and **c** HBPBI-15-30 membranes

sites for the formation of additional apatite during the subsequent SBF soaking.

The FTIR-ATR spectra in Fig. 3 provide direct evidence for the formation of apatite on the amino-terminated HBPBI membranes. Characteristic absorption bands related to the imidazole rings, can be observed at 1,630 cm^{-1} (–C=N– stretching vibration) and 1,413 cm^{-1} (in-plane deformation of imidazole rings). During the soaking process, phosphate vibration bands at 1,010–1,020 cm^{-1} gradually appeared, with increasing intensity. Simultaneously, typical absorption bands assigned to the amino-terminated HBPBI decreased to negligible levels after the immersion in SBF solution for 7 or 30 days. These results indicate that calcium phosphate was coated onto the amino-terminated HBPBI membrane. Additionally, carbonate bands (1,411 and 873 cm^{-1}) were observed in the FTIR-ATR spectrum of HBPBI-15, indicating the incorporation of carbonate ions into the apatite mineral [31]. These carbonates are also evident in the crystal structure of the layer [31], which exhibited an increase in the Ca/P ratio, up to 1.96 (see Supporting Information), which is significantly higher than the theoretical value of 1.67.

The crystal structure of the apatite coating was investigated before and after the various soaking steps. The XRD patterns in Fig. 4 show no discernable difference between the crystal structure of the bare HBPBI membrane and the same membrane after alternate soaking in Ca and P solutions. Only broad peaks, between 10° and 30° were

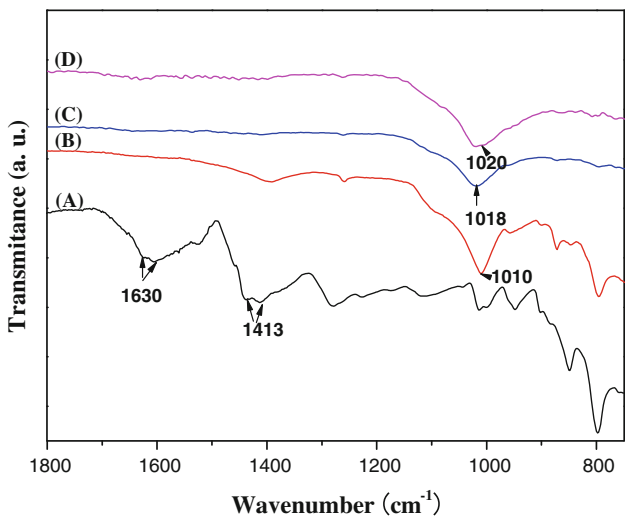

Fig. 3 FTIR-ATR spectra of (*a*) pure HBPBI, (*b*) HBPBI-15, (*c*) HBPBI-15-7 and (*d*) HBPBI-15-30 membranes

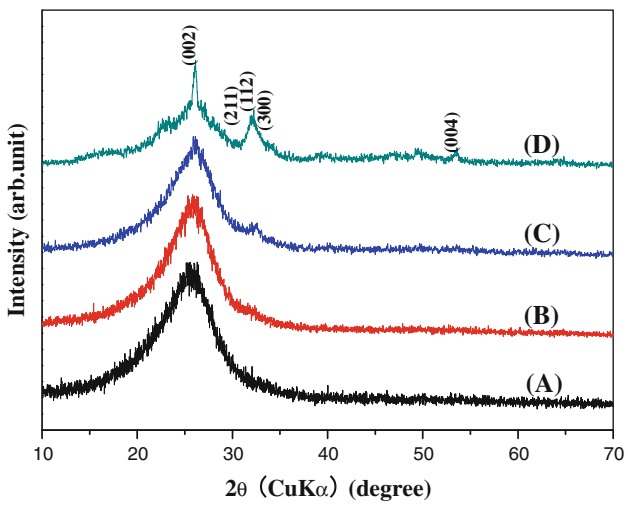

Fig. 4 XRD patterns obtained on (*a*) pure HBPBI, (*b*) HBPBI-15, (*c*) HBPBI-15-7 and (*d*) HBPBI-15-30 membranes

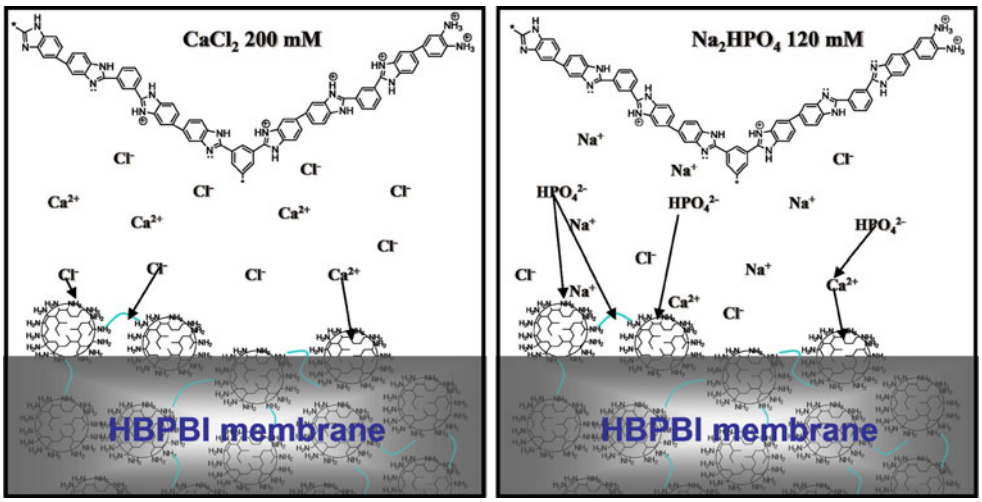

Scheme 3 Coating of apatite onto amino-terminated HBPBI membranes by an alternate soaking process

observed. However, electron diffraction (ED) experiments confirmed the existence of an apatite phase, containing small amount of amorphous calcium phosphate (ACP) and relatively large amounts of polycrystalline apatite. The inter-plane spacing of the diffuse diffraction rings are characteristic of apatite, which exhibits ED rings corresponding to the (002), (211) and (213) planes [32] (see Supporting Information). After soaking in SBF solution for 7 days, XRD peaks ranging from $2\theta = 31.8°$ to $2\theta = 32.9°$ became discernable, corresponding to the (211), (112), and (300) faces of apatite. Prolonging the duration of SBF soaking up to 30 days, enhanced the intensity of these characteristic peaks and produced additional peaks, also characteristic of apatite at $2\theta = 26.0°$ and $2\theta = 53.2°$.

4 Discussion

The above analyses indicate the formation of a dense and uniform apatite-like layer on amino-terminated HBPBI membranes after alternate soaking in Ca and P solution for 15 cycles. This apatite-like layer became a stable apatite phase by further soaking in an SBF solution. Although the nitrogenous groups of the amino-terminated HBPBI membranes are less active in cation adsorption than negatively charged groups, such as phosphates ($-PO_4H_2$) [19], sulfonic acids ($-SO_3H$) [13] and carboxylic acids (–COOH) [10, 20], an apatite layer was nevertheless created on the membrane surface. This may be attributable to the high density of amino, imine and imidazole groups at the membrane surface that facilitated apatite nucleation and growth [33].

These three nitrogenous functional groups play different roles in apatite growth due to their different degrees of protonation during the soaking process. The protonation of these groups is affected by both their pK_a and the pH of the surrounding solution. Both the amino groups and imine groups are protonated in the Ca and P solutions [34, 35]. A large proportion (about 90%) of imidazole groups ($pK_a = 6.99$) are protonated in the Ca solution (pH = 6.2). As the pH is increased to 9.3 in P solution, the imidazole groups deprotonate [36]. Thus, in the Ca solution (Scheme 3), only a small proportion (about 10%) of neutral imidazole groups would be able to form coordinating bonds with Ca^{2+} [37] to form apatite-like precursors. Electrostatic repulsion would prevent ionic interactions with other protonated groups in the membrane thereby decreasing the rate of apatite formation, relative to that on a negatively charged surface. In the next stage of the alternate soaking process, this membrane was then immersed in P solution (Scheme 3). The protonated amino and imine groups may then electrostatically adsorb HPO_4^{2-}. This interaction would simultaneously produce an apatite-like structure with the Ca^{2+} that had been coordinated by the imidazole groups in the first soaking phase. The adsorbed HPO_4^{2-} would then electrostatically bind Ca^{2+} in the next cycle and so on. Thus, the different nitrogenous functional groups each interact differently with Ca^{2+} and HPO_4^{2-} to contribute to the formation of the apatite coating [21].

Apatite has the lowest solubility of all calcium phosphates in aqueous solution at neutral pH value [38], making the SBF solution an ideal environment for forming stable apatite phase. The apatite-like precursor grown on the amino-terminated HBPBI membranes during the alternate soaking process was transformed into a more stable apatite phase by soaking in the SBF solution [38, 39]. This transformation was evidenced by the increase in apatite diffraction peak intensities in the XRD patterns (Fig. 4), and the reduction of imidazole peak intensities in the FTIR-ATR spectra (Fig. 3). Moreover, the thickness of the apatite layers increased with increasing immersion time in the SBF solution. Small flower-like clusters on the surface of

apatite-like layers acted as secondary nucleation sites for further apatite growth in the SBF solution, resulting in large globular particles on the membrane surface [38]. Additionally, the boundaries between the flower-like clusters and globular particles may induce apatite growth due to high stress force.

5 Conclusions

Apatite-like layers were coated onto amino-terminated hyperbranched polybenzimidazole membranes by two different soaking processes. Nitrogenous functional groups (amino, imide and imidazole groups) acted as active sites for the growth of apatite-like layers and the high densities of these groups facilitated apatite mineralization. The interactions between these and Ca^{2+} or HPO_4^{2-} were influenced by both their respective pK_a values and the pH of the soaking solution. Subsequent soaking in an SBF solution helped the apatite-like precursor layers to densify and kinetically stabilized the apatite phase.

Acknowledgments This work was supported by the National Natural Science Foundation of China (No. 50973062), Chinese High Tech Research and Development (863) Program (No. 2006AA02A108) and the Zhejiang Health Science Foundation (No. 2005A027).

References

1. Ohtsuki C, Kamitakahara M, Miyazaki T. Coating bone-like apatite onto organic substrates using solutions mimicking body fluid. J Tissue Eng Regen Med 2007;1:33–8.
2. Kamitakahara M, Ohtsuki C, Miyazaki T. Coating of bone-like apatite for development of bioactive materials for bone reconstruction. Biomed Mater. 2007;2:17–23.
3. Miyazaki T, Ohtsuki C, Akioka Y, Tanihara M, Nakao J, Sakaguchi Y, et al. Apatite deposition on polyamide films containing carboxyl group in a biomimetic solution. J Mater Sci Mater Med 2003;14:569–74.
4. Furuzono T, Taguchi T, Kishida A, Akashi M, Tamada Y. Preparation and characterization of apatite deposited on silk fabric using an alternate soaking process. J Biomed Mater Res. 2000;50:344–52.
5. Liu Y, Layrolle P, de Bruijin J, van Blitterswijk C, de Groot K. Biomimetic coprecipitation of calcium phosphate and bovine serum albumin on titanium alloy. J Biomed Mater Res. 2001;57:327–35.
6. Takeuchi A, Ohtsuki C, Kamitakahara M, Ogata S, Miyazaki T, Tanihara M. Biomimetic deposition of hydroxyapatite on a synthetic polypeptide with β sheet structure in a solution mimicking body fluid. J Mater Sci Mater Med. 2008;19:387–93.
7. Song J, Malathong V, Bertozzi RC. Mineralization of synthetic polymer scaffolds: a bottom-up approach for the development of artificial bone. J Am Chem Soc. 2005;127:3366–72.
8. Yamaguchi I, Itoh S, Suzuki M, Osaka A, Tanaka J. The chitosan prepared from crab tendons: II. The chitosan/apatite composites and their application to nerve regeneration. Biomaterials. 2003;24:3285–92.
9. Verma D, Katti K, Katti D. Bioactivity in in situ hydroxyapatite-polycaprolactone composites. J Biomed Mater Res A. 2006;78:772–80.
10. Oyane A, Uchida M, Choong C, Triffitt J, Jones J, Ito A. Simple surface modification of poly(ε-caprolactone) for apatite deposition from simulated body fluid. Biomaterials. 2005;26:2407–13.
11. Yokoyama Y, Oyane A, Ito A. Biomimetic coating of an apatite layer on poly(l-lactic acid); improvement of adhesive strength of the coating. J Mater Sci Mater Med. 2007;18:1727–34.
12. Gultekin N, Tihminlioglu F, Ciftcioglu R, Ciftcioglu M, Harsa S. Preparation and characterization of polylactide-hydroxyapatite biocomposites. Eur Ceram. 2004;264–268:1953–6.
13. Takahiro K, Ohtsuki C, Kamitakahara M, Miyazaki T, Tanihara M, Sakaguchi Y, et al. Coating of an apatite layer on polyamide films containing sulfonic groups by a biomimetic process. Biomaterials. 2004;25:4529–34.
14. Wang X, Li Y, Wei J, de Groot K. Development of biomimetic nano-hydroxyapatite/poly(hexamethylene adipamide) composites. Biomaterials. 2002;23:4787–91.
15. Oyane A, Kawashita M, Nakanishi K, Kokubo T, Minoda M, Miyamoto T, et al. Bonelike apatite formation on ethylene-vinyl alcohol copolymer modified with silane coupling agent and calcium silicate solutions. Biomaterials. 2003;24:1729–35.
16. Taguchi T, Muraoka Y, Matsuyama H, Kishida A, Akashi M. Apatite coating on hydrophilic polymer-grafted poly(ethylene) films using an alternate soaking process. Biomaterials. 2001;22:53–8.
17. Bajpai KA, Singh R. Study of biomineralization of poly(vinyl alcohol)-based scaffolds using an alternate soaking approach. Polym Int. 2007;56:557–68.
18. Arcos D, Ragel VC, Vallet-Regm M. Bioactivity in glass/PMMA composites used as drug delivery system. Biomaterials. 2001;22:701–8.
19. Kato K, Eika Y, Ikada Y. Deposition of hydroxyapatite thin layer onto a polymer surface carrying grafted phospahte polymer chain. J Biomed Mater Res. 1996;32:687–91.
20. Kawashita M, Nakao M, Minoda M, Kim HM, Beppu T, Miyamoto T, et al. Apatite-forming ability of carboxyl group-containing polymer gels in a simulated body fluid. Biomaterials. 2003;24:2477–84.
21. Tanahashi M, Matsuda T. Surface functional group dependence on apatite formation … in a simulated body fluid. J Biomed Mater Res. 1997;34:305–15.
22. Toworfe GK, Composto RJ, Shapiro IM, Ducheyne P. Nucleation and growth of calcium phosphate on amine-, carboxyl- and hydroxyl-silane self-assembled monolayers. Biomaterials. 2006;27:631–42.
23. Miyazaki T, Imamura M, Ishida E, Ashizuka M, Ohtsuki C. Apatite formation abilities and mechanical properties of hydroxyethylmethacrylate-based organic–inorganic hybrids incorporated with sulfonic groups and calcium ions. J Mater Sci Mater Med. 2009;20:157–61.
24. Song J, Malathong V, Bertozzi RC. Mineralization of synthetic polymer scaffolds: a bottom-up approach for the development of artificial bone. J Am Chem Soc. 2005;127:3366–72.
25. Yamaguchi I, Itoh S, Suzuki M, Osaka A, Tanaka J. The chitosan prepared from crab tendons: II. The chitosan/apatite composites and their application to nerve regeneration. Biomaterials. 2003;24:3285–92.
26. Pecheva E, Pramatarova L, Altankov G. Hydroxyapatite grown on a native extracellular matrix: initial interactions with human fibroblasts. Langmuir. 2007;23:9386–92.
27. Takahiro K, Chikara O, Masanobu K, Masao T, Toshiki M, Yoshimitsu S, et al. Removal of formaldehyde by hydroxyapatite layer biomimetically deposited on polyamide film. Environ Sci Technol. 2006;40:4281–5.

28. Xu H, Chen K, Guo X, Fang J, Yin J. Synthesis of hyperbranched polybenzimidazoles and their membrane formation. J Membr Sci. 2007;288:255–60.
29. Xu H, Chen K, Guo X, Fang J, Yin J. Synthesis and properties of hyperbranched polybenzimidazoles via $A_2 + B_3$ approach. J Polym Sci Polym Chem. 2007;45:1150–8.
30. Kokubo T, Takadama H. How useful is SBF in predicting in vivo bone bioactivity? Biomaterials. 2006;27:2907–15.
31. Leeuwenburgh SCG, Wolke JGC, Schoonman J, Jansen JA. Influence of precursor solution parameters on chemical properties of calcium phosphate coatings prepared using electrostatic spray deposition (ESD). Biomaterials. 2004;25:641–9.
32. Kim HM, Himeno T, Kokubo T, Nakamura T. Process and kinetics of bonelike apatite formation on sintered hydroxyapatite in a simulated body fluid. Biomaterials. 2005;26:4366–73.
33. Yokoyama Y, Oyane A, Ito A. Biomimetic coating of an apatite layer on poly(l-lactic acid); improvement of adhesive strength of the coating. J Mater Sci Mater Med. 2007;18:1727–34.
34. Bordwell FG, Algrim D, Vanier DR. Acidities of anilines and toluenes. J Org Chem. 1977;42:1817–9.
35. Bordwell FG. Equilibrium acidities in dimethyl sulfoxide solution. Acc Chem Res. 1988;21:456–63.
36. Cao P, Gu R, Tian Z. Surface-enhanced Raman spectroscopy studies on the interaction of imidazole with a silver electrode in acetonitrile solution. J Phys Chem B. 2003;107:769–77.
37. Schachschal S, Pich A, Adler HJ. Aqueous microgels for the growth of hydroxyapatite nanocrystals. Langmuir. 2008;24:5129–34.
38. Elliot JC. Structure and chemistry of the apatites and other calcium phosphates. Amsterdam: Elsevier Science BV; 1994.
39. Koutsopoulos S. Synthesis and characterization of hydroxyapatite crystals: a review study on the analytical methods. J Biomed Mater Res. 2002;62:600–12.